Miniring approach for high-throughput drug screenings in 3D tumor models

Nhan Phan[1,2], Bobby Tofig[3], Jin Huang[4], Sanaz Memarzadeh[4-8], Robert Damoiseaux[3,9] and Alice Soragni[1,8*]

[1]Division of Hematology-Oncology, Department of Medicine, David Geffen School of Medicine, University of California Los Angeles, CA, 90095

[2]Laboratory of Stem Cell Research and Application, University of Science, Vietnam National University, HCM City, Vietnam

[3]Molecular Screening Shared Resource, California NanoSystems Institute, University of California Los Angeles, CA 90095

[4]Department of Obstetrics and Gynecology, David Geffen School of Medicine, University of California Los Angeles, CA, 90095

[5]Eli and Edythe Broad Center of Regenerative Medicine and Stem Cell Research, University of California Los Angeles, CA 90095

[6]The VA Greater Los Angeles Health Care System, Los Angeles, CA, 90073

[7]Department of Biological Chemistry, University of California Los Angeles, CA 90095

[8]Molecular Biology Institute, University of California Los Angeles, CA 90095

[9]Department of Molecular and Medicinal Pharmacology, David Geffen School of Medicine, University of California Los Angeles, CA, 90095

* Correspondence to AS (alices@mednet.ucla.edu)

Abstract

There is increasing interest in developing 3D tumor organoid models for drug development and personalized medicine approaches. While tumor organoids are in principle amenable to high-throughput drug screenings, progress has been hampered by technical constraints and extensive manipulations required by current approaches. Here, we introduce a miniaturized, fully automatable, flexible high-throughput method using a simplified geometry to establish 3D organoids from cell lines and primary tumors and robustly assay drug responses.

Main Text

Preclinical drug development and discovery has relied heavily on traditional 2D cell culture methods. Nevertheless, 3D cancer models are a better approximation of the tumor of origin in terms of cell differentiation, microenvironment, histoarchitecture and drug response[1-8]. Various methods to set up tumor spheroids or organoids have been proposed, including using U-bottom low attachment plates, feeding layers or various biological and artificial matrices[2-3, 6, 9-15]. Methods such as low-attachment U-bottom plates ideally only carry one organoid per well, have limited automation and final assay capabilities[9-10, 15]. In addition, not all cells are capable of forming organized 3D structures with this method. Approaches that include a bio-matrix, such as Matrigel, have the potential to offer a scalable alternative in which cancer cells thrive[2,8,16-17]. However, several approaches so far rely on thick volumes of matrix which is not cost-effective, potentially hard for drugs to efficiently penetrate and difficult to dissolve fully at the end of the experiment[17]. In other applications, organoids are first formed and then transferred to different plates for drug treatment or final readout which can result in the tumor spheres sticking to plastic or breaking[8,16]. In other studies, assays are performed by disrupting the organoids to single cell suspensions at the end of the experiment[12-13]. All these manipulations introduce significant variability limiting applicability in screening efforts[6].

To circumvent these issues, we optimized an assay system for 3D organoid high-throughput drug screenings that is low cost, simple, robust, requires few cells and is easily automated. Our strategy takes advantage of a specific geometry and can be performed using regular plates, without any need to transfer the samples at any time or dissociating the pre-formed tumor organoids. Single cell suspensions are pre-mixed with cold Matrigel (3:4 ratio) and 10 μl of this mixture is plated in a ring shape around the rim of the wells of a 96 well plate (**Fig. 1a**). The Matrigel rapidly solidifies upon short incubation at 37°C (**Fig. 1a**). The combination of small volume and surface tension holds the cells in place until the Matrigel solidifies and prevents 2D growth at the center of the wells. As such, further media removal, changes of conditions or treatment addition can be easily performed pipetting in the center of the well, preventing any disruption of the gel or need to pipette organoids. Cancer cell lines grown in the miniring format give rise to organized tumor organoids that recapitulate features of the original histology (**Fig 1b and S1; Table S1**). The miniring approach is also suitable to establish patient-derived tumor organoids (PDTOs). Primary patient samples grow and maintain the heterogeneity of the original tumor as expected. As an example, Patient #1 PDTOs recapitulate features of high-grade serous carcinoma (HGSC) as well as clear cell tumor (**Fig. 1b**). Fewer than 5000 cells per well are sufficient to provide a quantifiable readout (**Fig. 1b**).

Next, we optimized a treatment protocol and readouts for the miniring approach. Our standardized paradigm includes: seeding cells on day 0, establishing organoids for 2-3 days followed by two consecutive daily treatments, each performed by complete medium change (**Fig. 1c**). Three drugs (ReACp53[12], Staurosporine and Doxorubicin) were tested at five concentrations in triplicates (**Fig. 1d-g**). We optimized different readouts so that the final assay can be adapted to the specific research question or instrument availability. After seeding cells in standard white plates, we performed a luminescence-based ATP assay to obtain a metabolic readout of cell status, calculate EC_{50} and identify cell-specific sensitivities (**Fig. 1, S2 and S3**). Results show how the Matrigel in the miniring setup is thin enough to

allow penetration not only of small molecules but also of higher molecular weight biologics such as peptides[12]. We performed two consecutive treatments which allows the drugs to not only penetrate the gel but also reach organoids that may be bulky[12]. However, the assay is flexible and can be easily adapted to single drug treatments followed by longer incubations, multiple consecutive recurring treatments, multi-drug combinations or other screening strategies (**Fig. S3**).

We also implemented assays to quantify drug response by measuring cell viability after staining of live organoids with specific dyes followed by imaging. We optimized a calcein release assay coupled to propidium iodide (PI) staining and a caspase 3/7 cleavage assay (**Fig. 1e-g and S4**). Both are performed upon seeding the cells in standard black plates. Tumor organoids are stained with the reagents after dispase release and neutralization. After a 30-45 minutes incubation, organoids are imaged with a Celigo S cell imager. Images are then segmented and quantified (**Fig. 1e-g and S4**). As the organoids are assayed in the same well in which they are seeded, it is important to determine which assay/plate to use beforehand. Although the assays are testing different biological events, results are concordant across the methods for the three molecules we tested (**Fig. 1, S4 and S5**).

Most importantly, the miniring approach offers the possibility to perform multiple assays on the same plate/set of samples. For example, we coupled the ATP metabolic assay to 3D tumor count and total area measurement. We did so while testing suitability of the approach to identify drug susceptibilities of primary ovarian cancer samples obtained from the operating room. We used one patient-derived cell line, S1 GODL[18], to optimize conditions (**Fig. S5**) and two ovarian cancer patient samples (**Table S1 and Fig. 2**). We optimized the initial seeding cell number and selected 5000 cells/well in order to obtain a low enough number of organoids for size distribution analysis but sufficient to measure an ATP signal by CaspaseGlo 3D. We prepared six 96 well plates and tested 252 different kinase inhibitors at two different concentrations for each patient (120 nM and 1 μM). We used the same experimental paradigm optimized above. All steps (media change, drug treatment) were automated and performed in less than 2 minutes/plate using a Beckman Coulter Biomek FX integrated into a Thermo Spinnaker robotic system. At the end of the experiment, PDTOs were first imaged in brightfield mode for organoid count/size distribution analysis followed by ATP assay. We observed a high degree of equivalence between outcomes from the two methods (**Fig. 2a and c**). Results highlight individual sensitivities to different drugs (**Fig. 2a-g**). The three samples tested showed minimal overlap in their response to kinase inhibitors (**Fig. 2g**).

Cells obtained from Patient #1 at the time of cytoreductive surgery[18] were chemo-naïve, and the heterogeneous nature of this clear cell/HGSC tumor was fully recapitulated in the PDTOs (**Fig. 1b**). The organoids were sensitive to 16/252 molecules tested and responded mostly to a variety of cyclin-dependent kinase (CDK) inhibitors with a stronger response to inhibitors hitting CDK1/2 in combination with CDK 4/6 or CDK 5/9 (**Fig. 2a-c and S5b**). Interestingly, CDK inhibitors have found limited applicability in ovarian cancer therapy so far[19].

Based on the profiles of the CDK inhibitors tested and on the response observed (**Fig. S5b-c**), we selected four untested molecules to assay. We anticipated that Patient #1 should not respond to Palbociclib (targeting only CDK4/6) and THZ1 (CDK7) while expecting a response to JNJ-7706621 (CDK1/2/3/4/6) and AZD54338 (CDK1/2/9; **Fig. S5b-c**). However, we observed a strong response to THZ1 but no response to JNJ-7706621 (**Fig. 2h**). Interestingly, both THZ1 and BS-181 HCl specifically target CDK7, however Patient #1 PDTOs showed a strong response to the former but no response to the latter which could be attributed to the different activity of the two as recently observed in breast cancer[20].

Cells were obtained from Patient #2, a heavily pre-treated patient diagnosed with progressive, platinum-resistant HGSC (**Table S1**). PDTOs only showed a strong response to 3/252 drugs tested, with sensitivity to two of these

(BGT226, a PI3K/mTOR inhibitor and Degrasyn, a deubiquitinases inhibitor) shared with all other tested samples (**Fig. 2c, 2f and S5a**). Moderate responses (50-60% residual cell viability at 1 μM) were observed for EGFR inhibitors and we could detect high expression of EGFR at the plasma membrane of the tumor cells (**Fig. S5e**). Remarkably, Patient #2 PDTOs showed a very moderate response to our positive control, Staurosporine, a pan-kinase inhibitor with very broad activity[21]. The significant lack of response to multiple therapies observed for Patient #2 could be due to over-expression of efflux membrane proteins. Indeed, the PDTOs showed a high level of expression of ABCB1 (**Fig. 2i**). High-expression of the ATP-dependent detox protein ABCB1 is frequently found in chemoresistant ovarian cancer cells and recurrent ovarian patients' samples and has been correlated with poor prognosis[22,23].

In conclusion, the miniring approach can be a robust tool to standardize precision medicine efforts, given its ease of applicability to many different systems and drug screening protocols as well as limited cell requirement which allows testing of samples as obtained from biopsies/surgical specimens without the need for expansion. As demonstrated above, the method rapidly allowed to pinpoint drug sensitivities in tumor samples and allowed us to identify a tumor "fingerprint", with multiple inhibitors converging on a given pathway. Interestingly, many of the drugs identified in our screening do not have a specific, unequivocal biomarker or genomic signature predictive of response. Thus, patients may greatly benefit from PDTO testing prior to therapy selection[6,8,24].

Our strategy can be successfully used to test samples that do not easily grow as patient-derived xenografts (PDX) in vivo. In fact, Patient #1 cells injected in NSG mice (500K/mouse, 12 mice) did not give rise to detectable tumor masses over six weeks (data not shown). Complete automation, scalability to 384 well plates, and flexibility to use different supports beside Matrigel can further extend applicability of the miniring approach.

Figures:

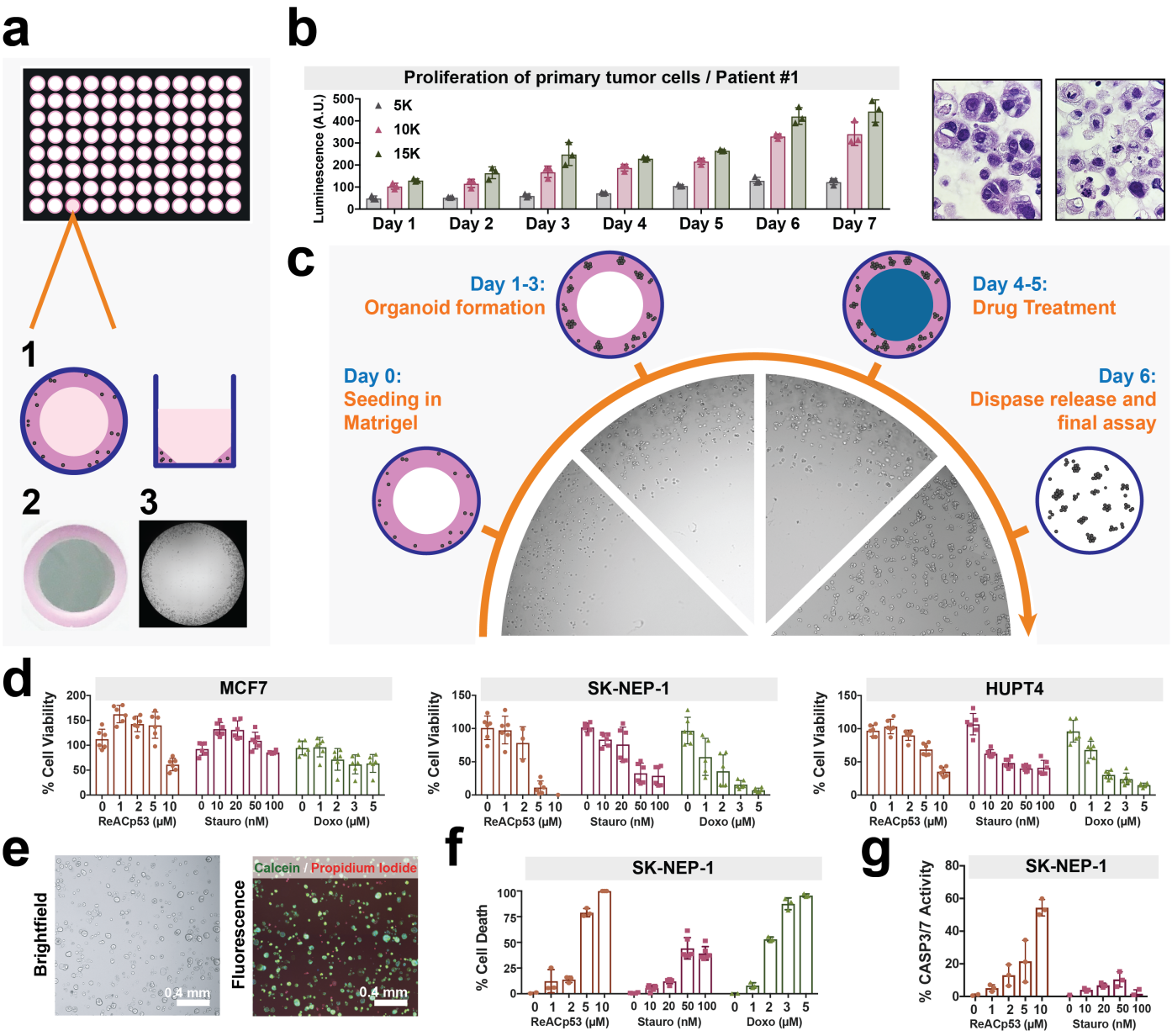

Figure 1. The miniring method for 3D tumor cell biology. (a) Schematics of the miniring setup. Cells are plated in Matrigel around the rim of the wells form a solid thin ring as depicted in 1 and photographed in 2, which has decreasing thickness. The picture in 3 acquired with a cell imager shows tumor organoids growing at the periphery of the well as desired, with no invasion of the center. **(b)** Proliferation of primary tumor cells as measured by ATP release. The miniring method allowed the patient sample to grow and maintain the heterogeneity and histology of the original ovarian tumor which had a high-grade serous carcinoma component (H&E left picture) and a clear cell component (H&E right picture). **(c)** Schematic of the drug-treatment experiments performed in the miniring setting. **(d - g)** Assays to monitor drug response of cell lines using the miniring configuration. Three drugs (ReACp53, Staurosporine and Doxorubicin) were tested at five concentrations in triplicates for all cell lines. **(d)** ATP release assay (CellTiter-Glo 3D) readout. **(e)** and **(f)** Calcein/PI readout. **(e)** Representative image showing staining of MCF7 cells with the dyes and segmentation to quantify the different populations (live / dead). **(f)** Quantification of Calcein/PI assay for three-drug assay. **(g)** Quantification of cleaved caspase 3/7 assay. Doxorubicin was omitted due to its fluorescence overlapping with the caspase signal.

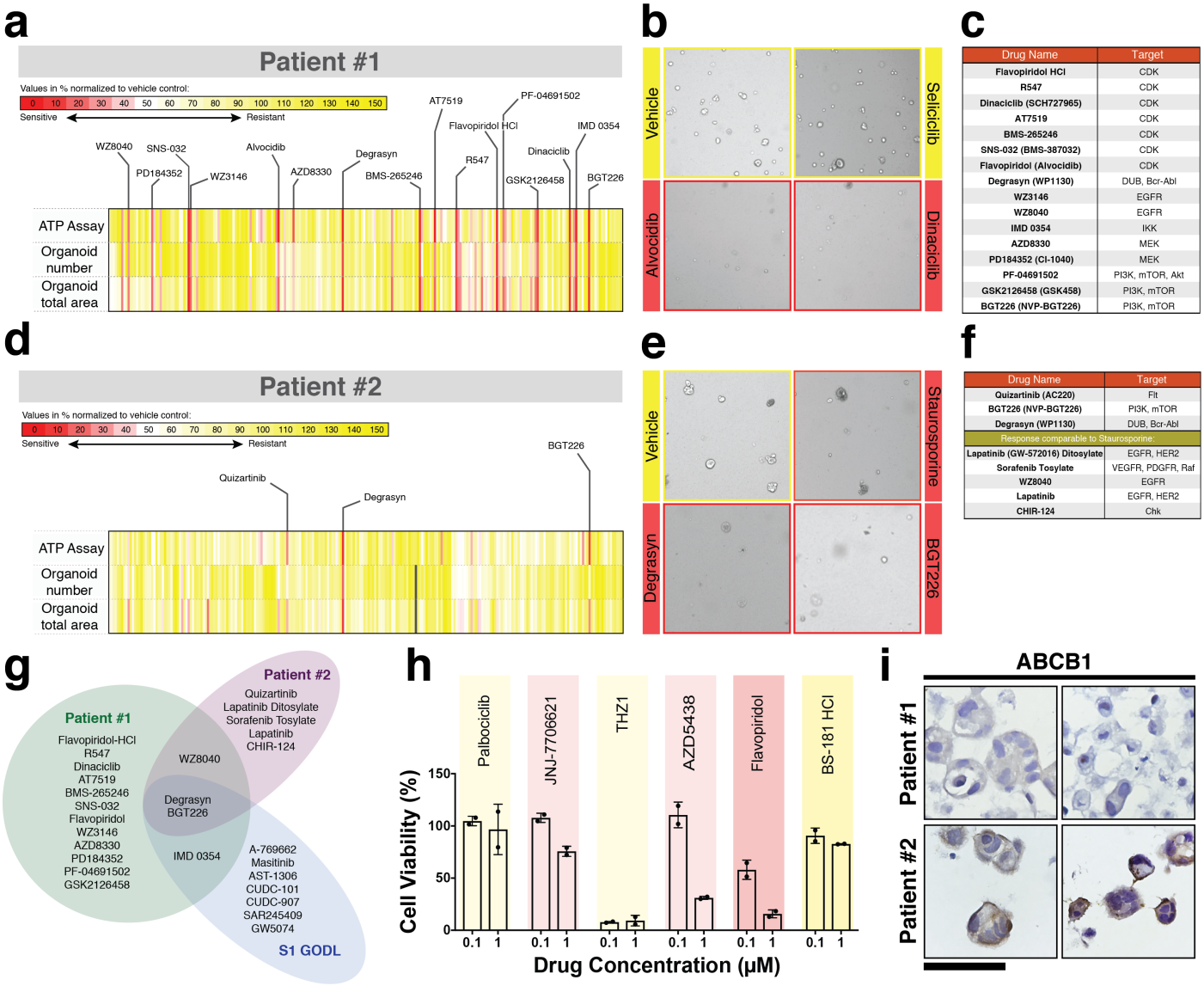

Figure 2. Miniring approach to unveil drug response patterns in PDTOs. (a) and **(d)** Results of kinase screening experiment. Two readouts were used for this assay: ATP quantification as measured by CellTiter-Glo 3D and organoids quantification evaluated by brightfield imaging. Brightfield images were segmented and quantified using the Celigo S Imaging Cell Cytometer Software. Both organoid number as well as total area were evaluated for their ability to capture response to drugs. In this plot, each vertical line is one drug, all 252 tested are shown. Values are normalized to the respective vehicle controls for each method and expressed as %. **(b)** and **(e)** A representative image of the effects of the indicated drug treatments as visualized by the cell imager. **(c)** and **(f)** Table of drug leads causing ≥ 75% cell death. For Patient #2, we included drugs inducing a response comparable to the Staurosporine control (~60% cell death). **(g)** Diagram illustrating limited overlap between the detected patterns of response identified through the miniring assay for Patients #1 and #2 and for the patient-derive line S1 GODL. **(h)** Small scale kinase assay on Patient #1 primary cells. ATP readout. Four molecules not present in the high-content screening were tested. We included two previously tested drugs, Flavopiridol and BS-181 HCl, as positive and negative control respectively. **(i)** Expression of the multi-drug efflux protein ABCB1 in PDTOs as visualized by IHC. Patient #2 expresses very high levels of the ABC transporter. Scale bar: 60 μm.

Acknowledgments

We thank Dr. Dylan Conklin (UCLA) and Dr. David Eisenberg (UCLA) for helpful discussions and inputs and the Translational Oncology Research Labs at UCLA for donating most cell lines. This project was supported by a Worldwide Cancer Research grant to AS (#16-0253). We acknowledge support by the Hirshberg Foundation (to AS), the UCLA SPORE in Prostate Cancer (NIH P50CA092131, PI: Robert Reiter) and a Jonsson Cancer Center Foundation Impact Award (to SM).

Author Contributions

AS and NP designed the project and carried out the experiments. SM procured the primary patient samples. JH contributed to feasibility experiments. BT and RB generated the kinase inhibitor drug library and optimized automation for primary sample assays. AS analyzed the data and wrote the paper with contributions from all authors.

References

1. Pickl, M. & Ries, C. H. Comparison of 3D and 2D tumor models reveals enhanced HER2 activation in 3D associated with an increased response to trastuzumab. *Oncogene* **28,** 461–468 (2008).
2. Katt, M. E., Placone, A. L., Wong, A. D., Xu, Z. S. & Searson, P. C. In Vitro Tumor Models: Advantages, Disadvantages, Variables, and Selecting the Right Platform. *Front Bioeng Biotechnol* **4**, 12 (2016).
3. Kimlin, L. C., Casagrande, G. & Virador, V. M. In vitro three-dimensional (3D) models in cancer research: an update. *Mol Carcinog* **52**, 167-182 (2013).
4. Tanner, K. & Gottesman, M. M. Beyond 3D culture models of cancer. *Sci Transl Med* **7,** 283ps9 (2015).
5. Nyga, A., Cheema, U. & Loizidou, M. 3D tumour models: novel in vitro approaches to cancer studies. *Journal of Cell Communication and Signaling* **5,** 239–248 (2011).
6. Fong, E. L. S., Toh, T. B., Yu, H. & Chow, E. K. 3D Culture as a Clinically Relevant Model for Personalized Medicine. *SLAS technology* **22**, 245-253 (2017).
7. Halfter, K. & Mayer, B. Bringing 3D tumor models to the clinic - predictive value for personalized medicine. *Biotechnol J* **12** (2017).
8. Pauli, C. *et al.* Personalized In Vitro and In Vivo Cancer Models to Guide Precision Medicine. *Cancer Discov* **7**, 462-477 (2017).
9. Friedrich, J., Seidel, C., Ebner, R. & Kunz-Schughart, L. A. Spheroid-based drug screen: considerations and practical approach. *Nat Protoc* **4**, 309-324 (2009).
10. Zanoni, M. *et al.* 3D tumor spheroid models for in vitro therapeutic screening: a systematic approach to enhance the biological relevance of data obtained. *Scientific reports* **6**, 19103 (2016).
11. Kelm, J. M., Timmins, N. E., Brown, C. J., Fussenegger, M. & Nielsen, L. K. Method for generation of homogeneous multicellular tumor spheroids applicable to a wide variety of cell types. *Biotechnol Bioeng* **83**, 173-180 (2003).
12. Soragni, A. *et al.* A Designed Inhibitor of p53 Aggregation Rescues p53 Tumor Suppression in Ovarian Carcinomas. *Cancer Cell* **29,** 90–103 (2016).
13. Boj, S. F. *et al.* Organoid models of human and mouse ductal pancreatic cancer. *Cell* **160**, 324-338 (2015).
14. Breslin, S., O'Driscoll, L. Three-dimensional cell culture: the missing link in drug discovery. Drug Discovery Today 18, 240–249 (2013).
15. Breslin, S., O'Driscoll, L. The relevance of using 3D cell cultures, in addition to 2D monolayer cultures, when evaluating breast cancer drug sensitivity and resistance. Oncotarget 7, 45745–45756 (2016).

16. Francies, H. E., Barthorpe, A., McLaren-Douglas, A., Barendt, W. J. & Garnett, M. J. Drug Sensitivity Assays of Human Cancer Organoid Cultures. *Methods Mol Biol* (2016).
17. Walsh, A. J. *et al.* Quantitative optical imaging of primary tumor organoid metabolism predicts drug response in breast cancer. *Cancer research* **74**, 5184-5194 (2014).
18. Janzen, D. M. *et al.* An apoptosis-enhancing drug overcomes platinum resistance in a tumour-initiating subpopulation of ovarian cancer. *Nature Communications* **6,** (2015).
19. Zhou, Q. Targeting Cyclin-Dependent Kinases in Ovarian Cancer. *Cancer Investigation* **0,** 1–10 (2017).
20. Li, B. *et al.* Therapeutic Rationale to Target Highly Expressed Cdk7 Conferring Poor Outcomes in Triple-Negative Breast Cancer. *Cancer Res* canres.2546.2016 (2017).
21. Belmokhtar, C. A., Hillion, J. & Ségal-Bendirdjian, E. Staurosporine induces apoptosis through both caspase-dependent and caspase-independent mechanisms. *Oncogene* **20,** 3354–3362 (2001).
22. Sun, S. *et al.* Prognostic Value and Implication for Chemotherapy Treatment of ABCB1 in Epithelial Ovarian Cancer: A Meta-Analysis. *PLoS One* **11,** (2016).
23. Vaidyanathan, A. *et al.* ABCB1 (MDR1) induction defines a common resistance mechanism in paclitaxel- and olaparib-resistant ovarian cancer cells. *Br J Cancer* **115,** 431–441 (2016).
24. Huang, L. *et al.* Ductal pancreatic cancer modeling and drug screening using human pluripotent stem cell and patient-derived tumor organoids. *Nat Med* **21,** 1364–1371 (2015).

Methods

Cell lines and primary samples: Cell lines are cultured in their recommended medium in the presence of 10% FBS (Life Technologies #10082-147) and 1% Antibiotic-Antimycotic (Gibco). DU145, PC3, PANC1 and HUTP4 were culture in DMEM (Life Technologies #1195-065). PAN03.27, MDA-MB-468 and MCF-7 was cultured in RPMI (Life Technologies #22400-089). SKNEP was cultured in McCoy medium (ATCC #30-2007). S1 GODL[1] and S9 GODL[2] cells are derived from HGSOC primary samples and cultured in RPMI. All treatments are performed in serum-free medium (PrEGM, Lonza #CC-3166).

Primary samples: Primary ovarian cancer specimens were dissociated to single cells and cryopreserved as previously described[1,2]. In short, fresh tumor specimens or ascites samples are obtained from consented patients (UCLA IRB 10-000727). Solid tumor specimens are minced, then enzymatically digested in 1 mg/ml collagenase and 1 mg/ml dispase. Digested tumors and ascites specimens are then treated with 0.05% Trypsin-EDTA. Trypsinization is stopped with DMEM/10% FBS, and the resulting cell suspension is filtered through a 40 µM cell strainer. Cells are cryopreserved in 90%FBS/10% DMSO.

Chemicals: Doxorubicin hydrochloride was purchased from Sigma (#44583). Staurosporine was purchased from Cell Signaling Technology (#9953S). ReACp53 was synthesized by GL Biochem and prepared as described[3].

3D organoids seeding/treatment procedure: Single-cell suspensions (2K-10K/well) were plated around the rim of the well of 96 well plates in a 3:4 mixture of PrEGM medium and Matrigel (BD Bioscience CB-40324). White plates (Corning #3610) were used for ATP assays while black ones (Corning #3603) were used for caspase or calcein assays. Plates are incubated at 37°C with 5% CO_2 for 15 minutes to solidify the gel before addition of 100 μl of pre-warmed PrEGM to each well using an EpMotion (Eppendorf). Two days after seeding, medium is removed and replaced with fresh PrEGM containing the indicated drugs. The same procedure is repeated twice in two consecutive days. 24h after the last treatments, media is removed and wells are washed with 100 μl of pre-warmed PBS. Organoids are then released from Matrigel for downstream experiments by 40 minutes of incubation in 50 μl of 5mg/mL dispase (Life Technologies #17105-041). All steps are performed with the EpMotion for small scale experiments and medium is removed/added from the center of the wells. For the high-throughput kinase screening experiment, we utilized a Beckman Coulter Biomek FX system with 96 channel head integrated into a Thermo Spinnaker robotic system with Momentum scheduling software. In short, an intermediary dilution plate (Axygen P-96-450V-C-S) was filled with 100 μl/well of media and pre-warmed to 37°C. Using pre-sterilized p50 tips, 1 μl of drug is transferred from a library compound plate to the intermediary media plate and thoroughly mixed. Next, the robot gently removed 100 μl of media from the matrigel/cell plate. The liquid handler was set up to hit the dead center of well with no contact to the Matrigel miniring. As a last step, the robot transferred 100 μl from the intermediary plate (media+drug) to the matrigel/cell plate. Media was easily dispensed without touching or disrupting the Matrigel miniring. The total process time outside of the CO_2 incubator was less than 2 so that the temperature was controlled throughout.

ATP assay: After the organoid release, 75 μl of Celltiter-Glo 3D Reagent (Promega #G968B) is added to each well followed by 1 minute of vigorous shaking. After a 30 minute incubation at room temperature and an additional minute of shaking, luminescence is measured with a SpectraMax iD3 (Molecular Devices) over 500 ms of integration time. Data is normalized to vehicle and plotted and EC_{50} are calculated with Prism 7. For the high-throughput drug screening, DMSO and Staurosporine (1 μM) are used as negative and positive control respectively. Values are normalized to vehicle. Hits are determined following two criteria: (1) cell death shows concentration-dependency and

(2) residual cell viability at 1 μM is ≤ 25%. For Patient #2, partial hits are defined as drugs giving response comparable to Staurosporine (50-60% residual viability at 1 μM).

Caspase 3/7/Hoechst assay: After dispase treatment, 100 μl of Nexcelom ViaStain™ Live Caspase 3/7 staining solution is added to each well. The staining solution consists of 2.5 μM Caspase reagent (Nexcelom #CSK-V0002) and 3 μg/ml Hoechst (Nexcelom #CS1-0128) in serum-free RPMI medium. Plates are incubated 37°C/5% CO_2 for 45 minutes and imaged with a Celigo S Imaging Cell Cytometer (Nexcelom). Data is normalized to vehicle values and plotted with Prism 7.

Calcein-AM/Hoechst/Viability assay: For this assay, 100 μl of Calcein-AM/Hoechst/PI viability staining solution are added to each well containing the released organoids. The staining solution includes the Calcein-AM reagent (Nexcelom CS1 #0119; 1:2000 dilution), Propidium Iodide (Nexcelom #CS1-0116; 1:500 dilution), Hoechst (Nexcelom #CS1-0126; 1:2500 dilution) in serum-free RPMI medium. Samples are incubated for 15 minutes at 37°C with 5% CO_2 before imaging with a Celigo S Imaging Cell Cytometer (Nexcelom).

Immunohistochemistry: Cells processed for fixation were seeded in 24 well plates to facilitate collection. Rings are washed with pre-warmed PBS, followed by 30 minute fixation at room temperature with 4% Formaldehyde EM-Grade (Electron Microscopy Science #15710). Samples are collected in a conical tube and centrifuged at 2000g for 10 minutes at 4°C. Pellets are washed with PBS followed by a second spin. After discarding the supernatant, pellets are mixed in 10 μl of HistoGel (ThermoScientific #HG-40000-012). The mixture is shortly incubated on ice for 5 minutes to solidify the pellets before transferring to a histology cassette for standard embedding and sectioning.

The slides are baked at 45°C for 20 minutes and de-paraffinized in xylene followed by ethanol washes and D.I. water. Endogenous peroxidases are blocked with by Peroxidazed-1 (Biocare Medical #PX968M) at RT for 5 minutes. Antigen retrieval is performed in a NxGEN Deloaking Chamber (Biocare Medical) using Diva Decloacker (Biocare Medical #DV2004LX) at 110°C for 15 minutes for Ki-67/Caspase-3 (Biocare Medical #PPM240DSAA) and pTEN (Cell Signaling Technology #CTS 9559) staining or using Borg Decloacker (Biocare Medical #BD1000 S-250) at 90°C for 15 minutes for Anti-P Glycoprotein (Abcam #EPR10364-57) staining. For EGFR staining, antigen retrieval is perfomed enzymatically with Carezyme III Pronase (Biocare Medical #PRT957) at 37°C for 5 minutes.

Blocking is performed at RT for 30 minutes with 8% Normal Goat Serum (Abcam #AB7841) in TBST for pTEN or using Background Punisher (Biocare Medical #BP947H) at RT for 15 minutes for the EGFR staining. Primary antibodies are diluted in Da Vinci Green Diluent (Biocare Medical #PD900L) for Anti-P Glycoprotein (1:300) and pTEN (1:100) incubated at 4°C overnight or Van Gogh Diluent (Biocare #PD902H) for EGFR (1:30) incubated at RT for 30 minutes. The combo Ki-67/Caspase-3 solution is pre-diluted and added to the sample for 60 minutes at room temperature. Secondary antibody staining is performed with Rabbit on Rodent HRP-polymer (Biocare Medical #RMR622G) for the Anti-P Glycoprotein and pTEN or with Mouse on Mouse HRP-polymer (Biocare Medical #MM620G) for EGFR. MACH 2 double Stain 2 (Biocare Medical #MRCT525G) is used for Ki-67/Caspase-3 combinatorial staining. All secondary antibodies are incubated at RT for 30 minutes.

Chromogen development is performed with Betazoid DAB kit (Biocare Medical #BDB2004) for Anti-P Glycoprotein, pTEN and EGFR and Ki-67 or Warp Red Chromogen Kit (Biocare Medical #WR806) for Caspase-3. The reaction is quenched by dipping the slides in D.I water. Hematoxylin-1 (Thermo Scientific #7221) is used for counterstaining. The slides are mounted with Permount (Fisher Scientific #SP15-100). Images are acquired with a Revolve Upright and Inverted Microscope System (Echo Laboratories).

Methods References:

1. Janzen, D.M., et al., An apoptosis-enhancing drug overcomes platinum resistance in a tumour-initiating subpopulation of ovarian cancer. Nat Commun, 2015. 6: p. 7956.

2. La, V., et al., Birinapant sensitizes platinum resistant carcinomas with high levels of cIAP to carboplatin therapy. NPJ Precision Oncology, 2017. In press.

3. Soragni, A. *et al.* A Designed Inhibitor of p53 Aggregation Rescues p53 Tumor Suppression in Ovarian Carcinomas. *Cancer Cell* **29,** 90–103 (2016).

SUPPLEMENTARY MATERIAL

Mini-ring approach for high-throughput drug screenings in 3D tumor models

Nhan Phan, Bobby Tofig, Jin Huang, Sanaz Memarzadeh, Robert Damoiseaux and Alice Soragni

Supplementary Table:

Stable Lines:

Specimen	Tumor Classification	Base Medium
MCF7	Invasive breast ductal carcinoma	RPMI
MD-MBA-468	Breast adenocarcinoma	RPMI
PANC1	Pancreatic ductal adenocarcinoma	DMEM
PANC03.27	Pancreatic adenocarcinoma	RPMI
HUPT4	Pancreatic adenocarcinoma	DMEM
PC3	Prostatic adenocarcinoma	DMEM
DU145	Prostatic carcinoma	DMEM
SK-NEP-1	Ewing sarcoma	McCoy
S1 GODL	High-grade serous ovarian carcinoma	RPMI
S9 GODL	High-grade serous ovarian carcinoma	RPMI

Primary Specimens:

Specimen	Tumor Classification	Sample Type	Therapy
Patient #1	Metastatic clear cell and high grade serous cancer with a 60% clear cell and 40% HGSC component	Ascites	None
Patient #2	High-grade serous ovarian carcinoma, Stage IIIC	Ascites	Carboplatin / Taxol / Avastin

Table S1. Characteristics of samples used in this study.

Supplementary Figures:

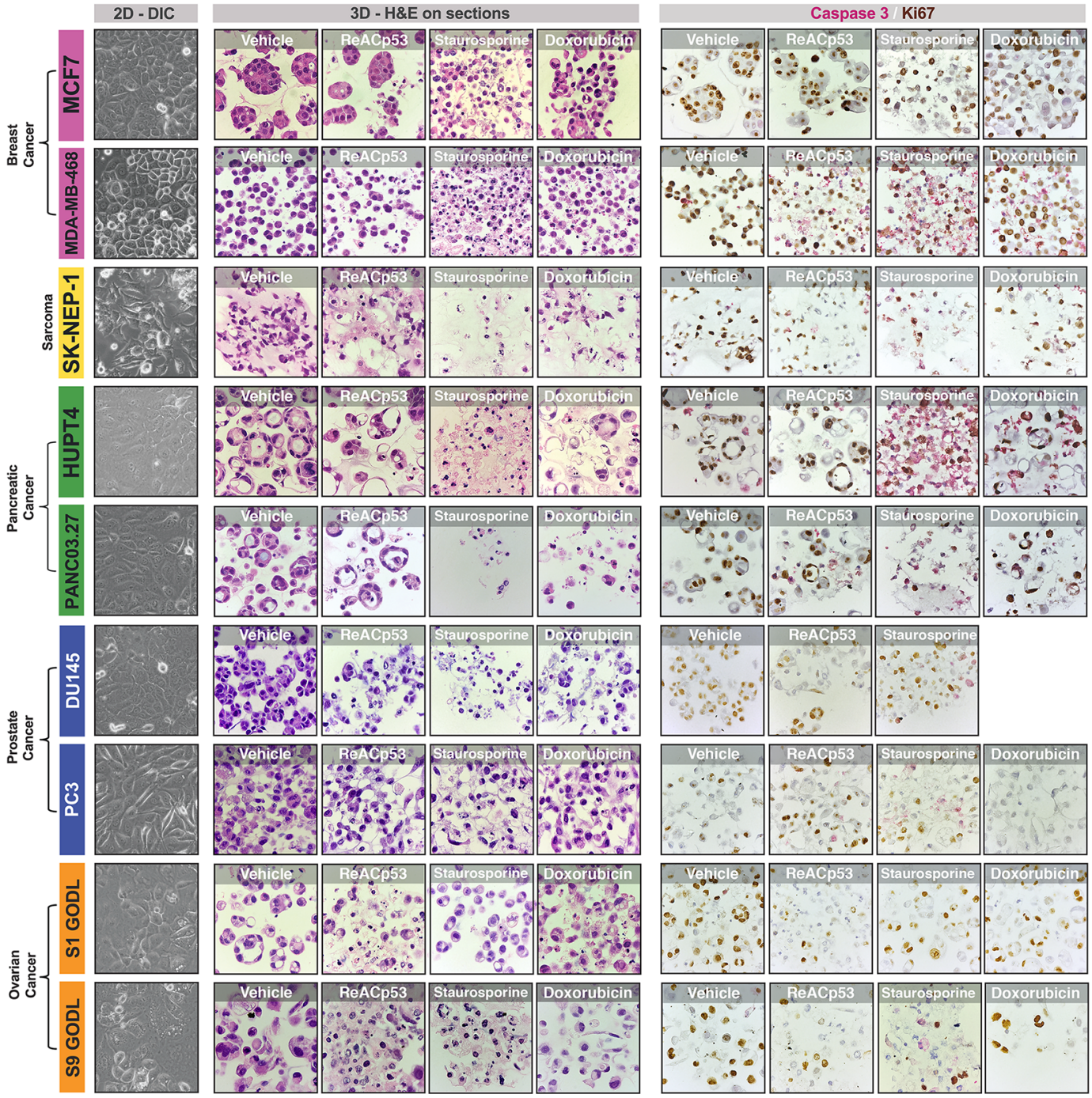

Figure S1. Morphology of 3D tumor models. Tumor cell lines used in this study grown in 3D processed for histology. The corresponding cells grown in 2D are shown on the left (40x magnification). On the right, H&E and Caspase/Ki67 staining on sections from embedded 3D tumor organoid samples (60x magnification).

a

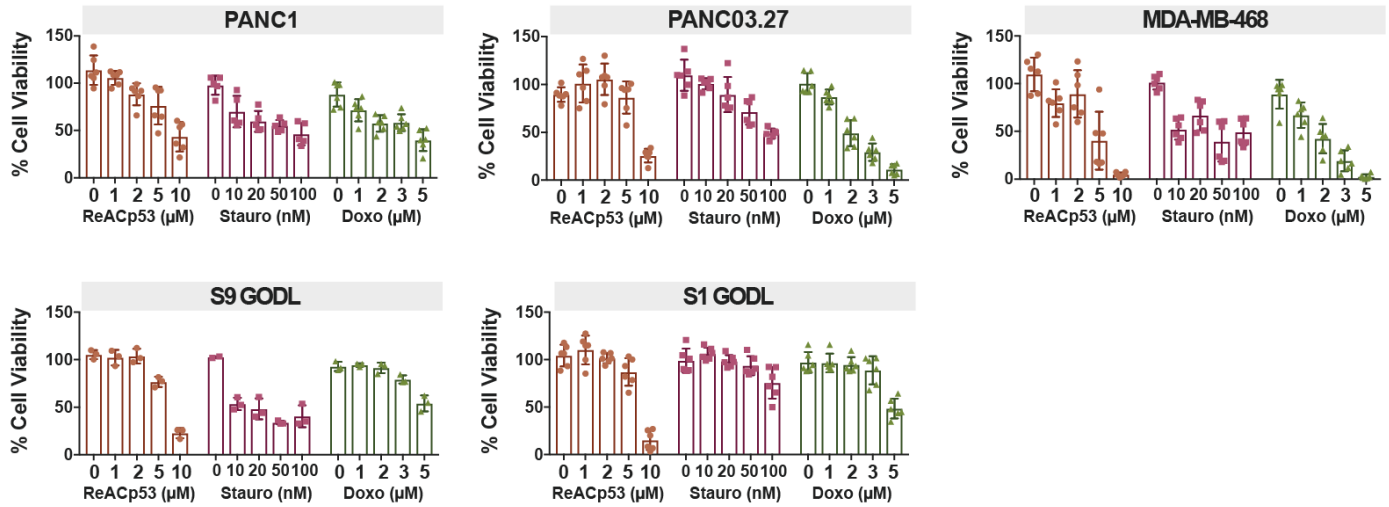

b

	ReACp53	Staurosporin	Doxorubicin
S1 GODL	6.9	0.2	5.0
S9 GODL	7.5	0.2	5.9
SKNEP	2.9	0.3	0.9
MCF7	9.9	0.1	12.0
HUPT4	7.4	0.3	1.5
PANC1	6.9	ND	5.7
PANC03.27	8.5	0.8	2.1
MDA-MB-468	2.5	ND	1.7

Figure S2. ATP readout and EC_{50} values for three-drug assay. (a) ATP quantification as measured by CellTiter-Glo 3D. Data from 2 independent experiments, n=3 for each are plotted. Error bars represent standard deviation; bars represent mean values. **(b)** EC_{50} values as calculate from the ATP quantification data. All values are expressed in μM.

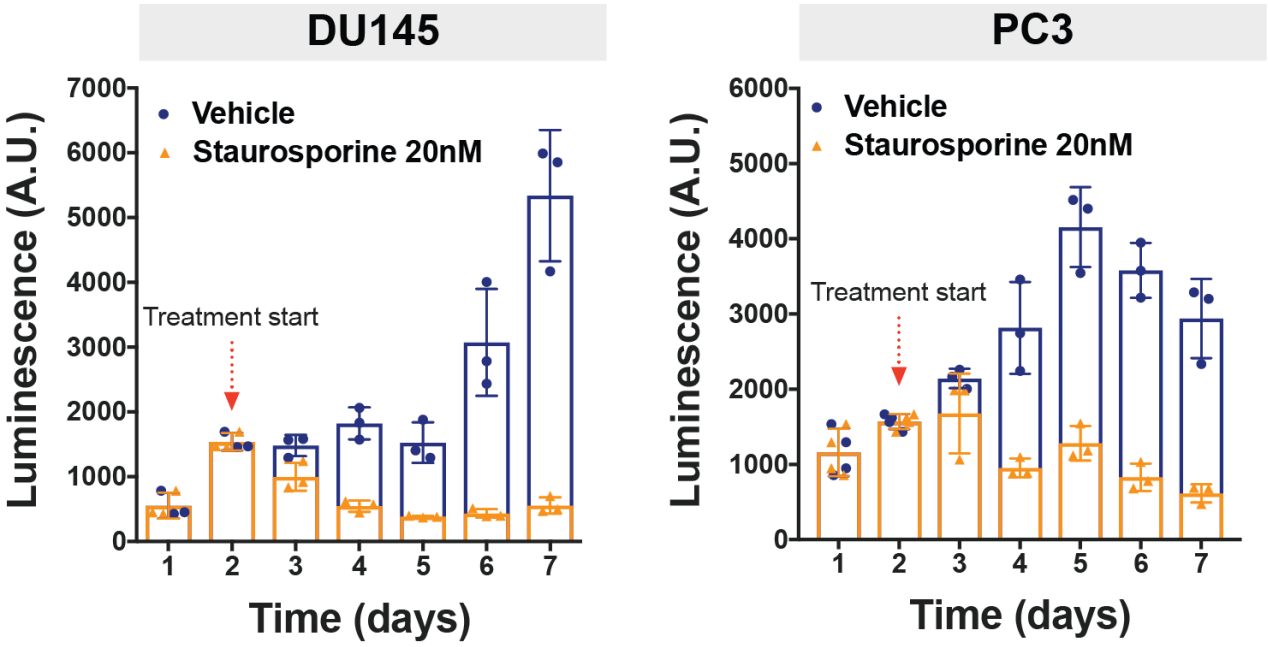

Figure S3. Adaptability of miniring assay to different treatment schedules. ATP quantification as measured by CellTiter-Glo 3D of prostate cancer organoids treated for 5 consecutive days with either vehicle or 20 nM Staurosporine.

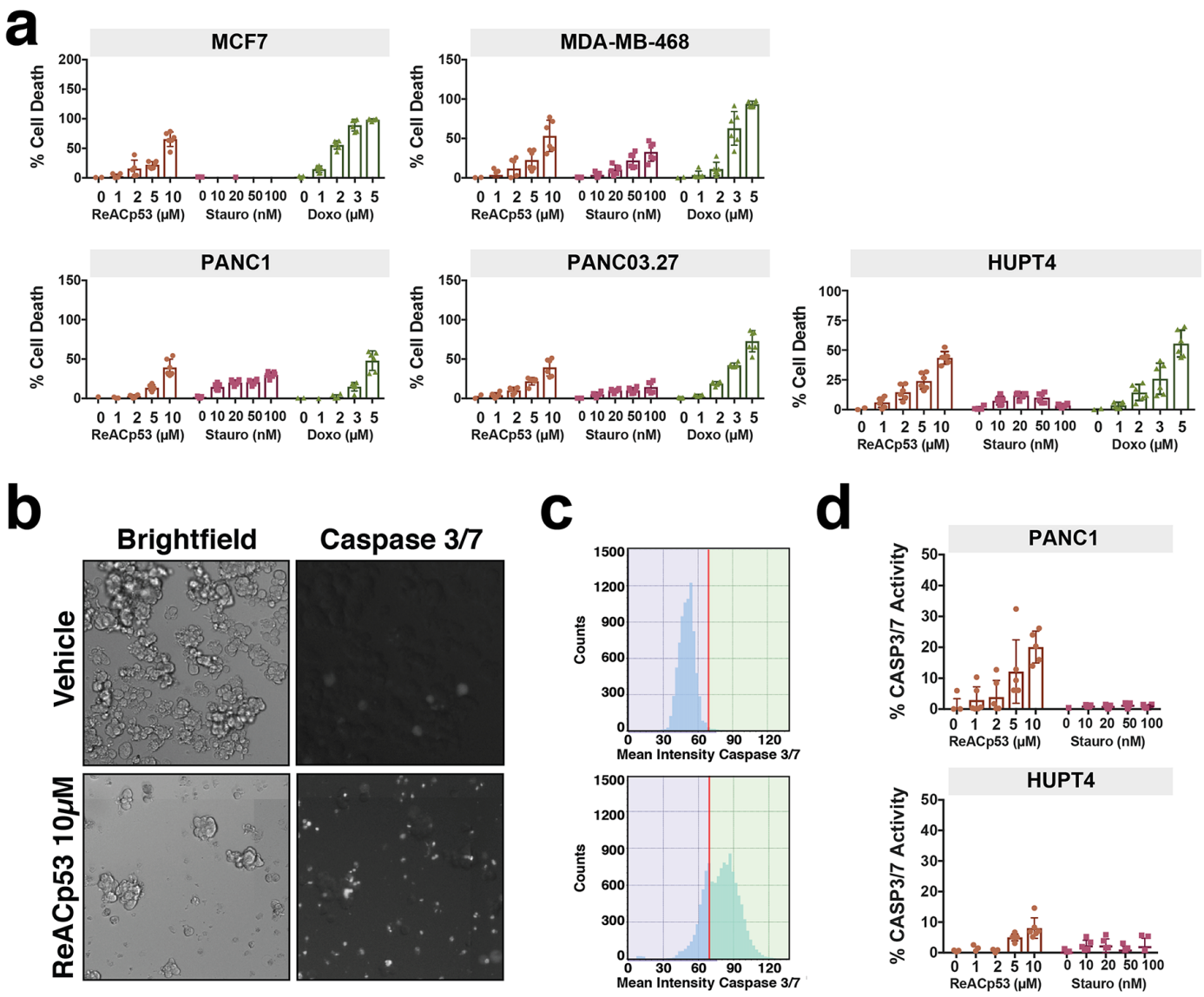

Figure S4. Additional optimized readouts for miniring assay (a) Quantification of the calcein release / PI uptake experiment. Two independent experiments shown, n=3 for each. Error bars are standard deviation while bars represent mean values. **(b)** and **(c)** Example of outcome for the caspase 3/7 cleavage experiment. DU145 prostate cancer cells are shown. A substrate becomes fluorescent when cleaved by caspase 3 or 7. Treatment induces high levels of caspase activation. Histograms of fluorescence intensity are shown in **(c)**. **(d)** Quantification of active caspase 3/7 activity normalized to control. Doxorubicin has intrinsic fluorescence that masks the caspase signal hence was excluded from this analysis.

a

Drug Name	Target
A-769662	AMPK
Masitinib (AB1010)	c-Kit, PDGFR, FGFR, FAK
Degrasyn (WP1130)	DUB, Bcr-Abl
AST-1306	Erb2, EGFR
CUDC-101	HDAC, HER2, EGFR
CUDC-907	HDAC, PI3K
IMD 0354	IKK
SAR245409 (XL765)	PI3K, mTOR
BGT226 (NVP-BGT226)	PI3K, mTOR
GW5074	Raf

b

Targets:	CDK1	CDK2	CDK3	CDK4	CDK5	CDK6	CDK7	CDK9	Other Targets
Flavopiridol (Alvocidib)	+++	+++		+++		+++	+		
R547	++++	++++		++++					GSK-3β
Dinaciclib (SCH727965)	++++	++++			++++			++++	
AT7519	++	++	+	++	+++	++	+	++++	GSK-3β
BMS-265246	++++	++++		++					
Flavopiridol (Alvocidib) HCl	+++	+++		+++		+++	+		
SNS-032 (BMS-387032)	+	+++		+	+		++	++++	GSK-3α,GSK-3β

c

Targets:	CDK1	CDK2	CDK3	CDK4	CDK5	CDK6	CDK7	CDK9	Other Targets
Roscovitine (Seliciclib,CYC202)		+			++				ERK2,GST-ERK1,ERK1
Milciclib (PHA-848125)	+	++		++	+		++		TrkA
PHA-793887	++	++++		++	++++		++++	++	GSK-3β
BS-181 HCl							+++		

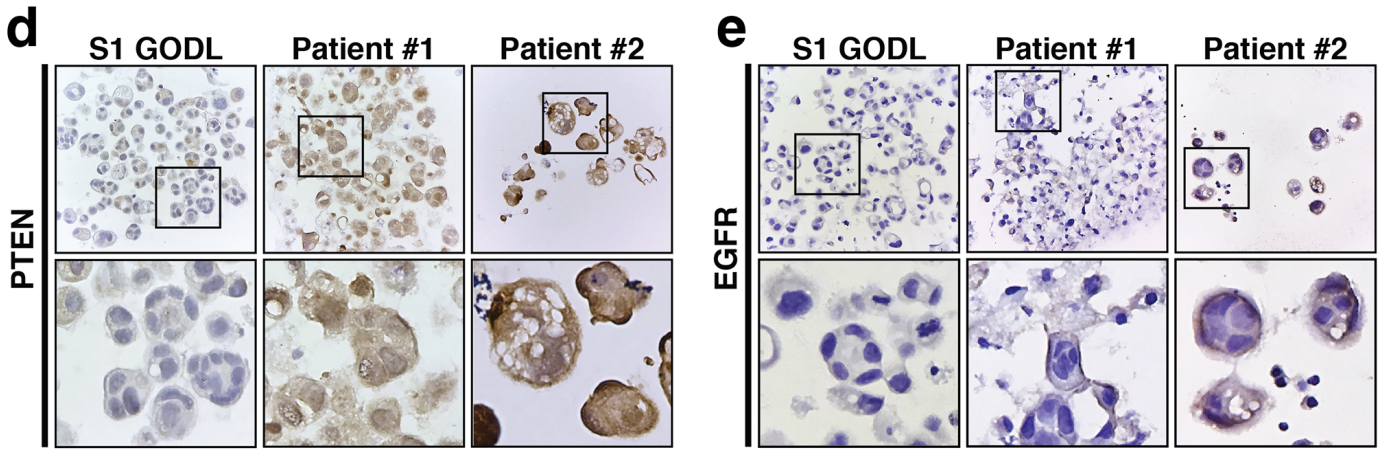

Figure S5. Results and validation of PDTO kinase screening. (a) Kinase inhibitors to which the HGSC control patient-derived line S1 GODL responded to. **(b)** List of CDK inhibitors that induced cell death in >75%Patient #1's organoids. Targets and specificity of each is listed. The patient responded to CDK inhibitors hitting CDK1/2 in combination with CDK 4/6 or CDK 5/9. **(c)** CDK inhibitors included in the 252-molecule screening that did not induce a response in Patient #1 organoids. The molecules share a low CDK1 targeting activity. **(d)** PTEN staining of S1 GODL, Patient #1 and Patient #2 organoids. **(e)** Expression of EGFR in S1 GODL, Patient #1 and Patient #2 3D tumors. Magnification: 40x.